Glycoconj J (2009) 26:1181–1195
DOI 10.1007/s10719-009-9238-9

Differences in the sialylation patterns of membrane stress proteins in chemical carcinogen-induced tumors developed in BALB/c and IL-1α deficient mice

Avi Avidan · Michal Perlmutter · Smadar Tal · Omer Oraki · Tsachi Kapp · Yacov Krelin · Moshe Elkabets · Shahar Dotan · Ron N. Apte · Rachel G. Lichtenstein

Received: 8 August 2008 / Revised: 6 March 2009 / Accepted: 6 April 2009 / Published online: 9 May 2009

Abstract We evaluated the patterns of sialylation on fibrosarcoma cell lines arising following 3-methylcholanthrene treatments of wild-type and IL-1α-deficient mice; the former induced progressive tumors, whereas the latter cell lines induced regressing tumors or failed to develop into tumors in mice due to immune rejection. In regressing tumors, terminating α2-6-Neu5Ac residues were present at lower levels than in progressively growing tumors. In both tumor cells, the amount of α2-6-Neu5Ac residues was higher by an order of magnitude relative to the amount expressed in primary fibroblasts harvested from IL-1α-deficient and wild-type mice. We focused on membrane proteins, which may interact with the immune system. Interestingly, HSP65, grp75, and gp96 were found on the surfaces of malignant cells and were shown to possess sialylated N-glycans. The amount of trisialylated glycans on gp96 and HSP65 and monosialylated glycans on grp75 of regressing cells was significantly lower than in progressively growing cells, suggesting a dependency of these specific glycoforms on anti-tumor immunity.

Keywords α2-6-Neu5Ac · Immunogenicity · IL-1α · Heat-shock proteins · Sialylated N-glycans

Abbreviations

DDW	double distilled water
Gal	galactose
GlcNAc	*N*-acetylglucosamine
gp96	96 kDa glycoprotein
grp	glucose regulated protein
HPLC	high performance liquid chromatography
HSP	heat shock protein
IFN	interferon
IL-1	interleukin 1
Man	mannose
3-MCA	3-methylcholanthrene
MHC	major histocompatibility class
Mw	molecular weight
Neu5Ac	*N*-acetylneuraminic acid
NK	natural killer
NKT	natural killer T
pI	isoelectric point
PNGase-F	*N*-glycosidase F
WT	wild-type

Introduction

Glycans, chains of sugars covalently linked to either proteins or lipids or found in free form, are assembled by glycosyltransferases and glycosidases in the secretory pathway. The combined actions of these enzymes lead to

This study is dedicated to the memory of Professor Shraga Segal

Electronic supplementary material The online version of this article (doi:10.1007/s10719-009-9238-9) contains supplementary material, which is available to authorized users.

A. Avidan · M. Perlmutter · S. Tal · O. Oraki · T. Kapp · R. G. Lichtenstein (✉)
Department of Biotechnology Engineering,
Faculty of Engineering and the Israeli Center for Glycobiology,
Ben-Gurion University of the Negev,
Beer-Sheva 84105, Israel
e-mail: ruha@bgu.ac.il

Y. Krelin · M. Elkabets · S. Dotan · R. N. Apte
Department of Microbiology and Immunology,
Faculty of Health Sciences and The Cancer Research Center,
Ben-Gurion University of the Negev,
Beer-Sheva 84105, Israel

a diverse array of glycoconjugates termed glycoforms. These glycans are frequently terminated by sialic acid residues, a process mediated by various sialyltransferases that can be distinguished by the glycan acceptor recognized and the linkage generated. Most classes of glycans are membrane-bound glycoconjugates or are secreted to the cell microenvironment, locations that enable glycans to interact with the immune system [1]. In addition, the contribution of glycans to the tumor microenvironment was described. Accordingly, aberrant patterns of cell glycosylation were shown to be correlated with tumor proliferation, invasion, metastasis, and angiogenesis, mainly by altering cell-to-cell or cell-to-matrix interactions and cell signaling and motility [2, 3]. Enhanced levels of cell surface Neu5Ac (sialic acid) residues frequently correlate with cancer progression, metastasis, invasion, and cell motility [4–6]. However, the mechanisms whereby cellular glycosylation affects tumor progression are not fully understood. Furthermore, the contribution of glycosylation changes, particularly sialylation, in determining the immunogenicity of malignant cells, remains obscure.

Recently, processes of immunoediting, in which immunity controls and shapes tumor cell immunogenicity, were described [7, 8]. It was shown that in mice deficient in cells or cytokines essential for the development of anti-tumor immunity, the overt tumors that develop following treatment with a carcinogen consist of immunogenic cells. In contrast, non-immunogenic tumors develop under the same experimental conditions in control mice. The roles of IL-1 molecules in the process of carcinogenesis have been studied by the Apte group, using mice deficient in genes encoding IL-1 agonists [9]. The IL-1 family includes two major agonistic molecules, IL-1α and IL-1β. In their soluble form, the two IL-1 molecules bind to the same signaling receptor, IL-1Ra, to exert the same biological response. However, in the *in vivo* context of the milieu of the producing cell, both IL-1α and IL-1β differ dramatically in their compartmentalization, likely dictating distinct functions. Studies of IL-1 deficient mice have demonstrated that host IL-1β deficiency reduces both the frequency of tumors that develop in mice following treatment with the carcinogen 3-MCA and the tumor invasiveness of transplantable cell lines, due to impaired local inflammatory responses [10]. By contrast, a deficiency of IL-1α at the site of carcinogen injection did not impair inflammatory responses or the frequency of tumors or their kinetics of development, which were similar to those observed in control mice. However, tumors that arose in IL-1$\alpha^{-/-}$ mice did not grow in intact mice and were shown to be immunogenic and rejected by immune mechanisms. These findings indicate that IL-1α is an important cytokine in the process of immunoediting [11]. We assume that during the immunoediting process, tumor cells bear aberrant glycans. Moreover, since IL-1 is involved in the metastasis and invasiveness of malignancies, we hypothesized that 3-MCA induced tumors developed in IL-1α deficient mice bear antigenic molecules lacking α2-6 Neu5Ac residues. By contrast, in control mice, the metastatic and invasive properties of tumors cause them to over-express α2-6 Neu5Ac residues. In this study, we estimated α2-6 sialylation, describing the specific expression of Neu5Ac residues on the cell surface heat shock proteins of immunogenic tumor cells arising in 3-MCA-treated IL-1$\alpha^{-/-}$ mice as compared to tumors obtained from WT mice treated with 3-MCA and that induce in vivo progressive growth. Heat shock proteins play a key role in different immunological phenomena. Nevertheless, it is poorly understood whether the glycoforms of these proteins play any role in the malignant process leading to the immune response against cancer. Here, we demonstrate differences in the amount of sialylation of HSP65, grp75, and gp96 between progressively-growing and non-invasive, immunogenic 3-MCA-induced fibrosarcoma cells. We believe that differences in the sialylation levels of heat shock proteins may affect their immunological properties.

Materials and methods

3-MCA-induced fibrosarcoma cell cultures

Two lines of 3-MCA induced fibrosarcoma cells from BALB/c mice and two lines from IL-1$\alpha^{-/-}$ mice were used in this study [10]. The cells were cultured in 180 cm^2 T-flasks, in 5% CO_2 and 99% humidity at 37°C. Dulbecco's modified Eagle's medium (DMEM), supplemented with 1% penicillin streptomycin, 1% L-glutamic acid, and 10% fetal bovine serum, was used. For flow cytometry analysis, cells were trypsinized with 3 ml of trypsin-EDTA, washed with medium, and then centrifuged at 2,000 rpm for 5 min at 4° C. The cells were suspended and placed in a polypropylene tube at 37°C, 99% humidity, and 5% CO_2, and they were subjected to gentle agitation conditions to let the membrane turnover. Cell number and viability were determined by Trypan Blue exclusion. For protein extraction, cells were harvested using a rubber policeman for mechanical dissociation when the flasks exhibited approximately ~80% cell confluence. The cells were washed twice in 10 ml ice-cold PBS. Cells from three flasks were pooled, centrifuged at 300×g for 7 min at 4°C, and stored at −20°C. After 3 days, their membranes or cytosolic proteins were extracted by a ProteoExtract kit (Calbiochem, San Diego, CA) and the presence of epidermal growth factor receptors (EGFRs) was revealed by anti-EGFR antibody binding (Santa Cruz Biotechnology, Santa Cruz, CA) and was used as a marker for protein membrane preparation.

Isolation of primary fibroblast cells

Two IL-1$\alpha^{-/-}$ and two WT mice were sacrificed. Their dorsal skin was shaved, cut into small pieces, and then stirred and incubated in HEPES buffer, pH 7.4, containing 200 U/ml of type IV collagenase for 40 min at 37°C. The resultant suspension was filtered through gauze to remove undigested tissue and then centrifuged at 1,000×g for 6 min. The supernatants were discarded and the isolated cells were resuspended in DMEM supplemented with 1% penicillin-streptomycin, 1% L-glutamic acid and 10% FBS and subsequently cultured in 50 cm^2 Petri dishes.

Analysis of glycan epitope expression

The expression of α-linked mannose, GlcNAc, and β-galactosyl residues strongly reactive to T-antigen, β-galactosyl residues strongly reactive to N- and O-glycans, and of α2-6-linked Neu5Ac on the surface of fibrosarcoma cells was examined by flow cytometric analysis (FACS) as previously described [12]. Briefly, cells (2.5×10^5) were blocked by a FACS solution of 1% bovine albumin in PBS for 1 h at 4°C, incubated with the fluorescent lectins (30 μg/ml, Vector laboratory, Burlingame, CA) concanavalin A (Con A), wheat germ agglutinin (WGA), peanut agglutinin (PNA), jacalin, ricinus communis agglutinin I (RCA-I) or sambucus nigra lectin (SNA) for 30 min at 4°C, washed and resuspended in 0.3 ml of FACS solution. The cells were then analyzed by FACSCalibor flow cytometry (BD Biosciences, San Jose, CA), operated with CellRequest software.

Quantification of glycosyltransferases

Glycosyltransferase mRNA expression was determined by quantitative real time PCR using cDNA specifically designed for the amplification of these mRNA species. RNA was extracted using the RNAeasy kit (QIAGEN, Hilden, Germany) and cDNA was synthesized using a reverse transcription system (Promega, Madison, WI). Oligo dT primer was used according to standard manufacturer protocol. Primers to the housekeeping gene, β-actin (5'- GGTCTCAAACATGATCTGGG-3' (forward); 5'-GGGTCAGAAGGATTCCTATG-3' (reverse)), were used as a standard to quantitate mRNA levels of α2, 3-Sialytransferase VI (ST3Gal VI) (primers: 5'- CCCAAA CACCCTACAACAGG -3' (forward) ;5'-TCAAAGA CATGGTGGCATTC-3' (reverse)), α2, 6-Sialytransferase III (ST6GalNAc III) (primers: 5'-AGTCACAGCCAT CAGGTCACT-3' (forward); 5'- CCCTGGACA TTCTCTGGTGT -3' (reverse)), α2, 6 Sialytransferase I (ST6Gal I) (primers: 5'-TGGGACATCATTCAGG AAATC-3' (forward); 5'- AAGAGGAGCGGATGGT AGG-3' (reverse)) and α1,3-Galctosyltransferase (α1, 3-GT) (primers: 5'-GATGCCAATGTGACCATCAG-3' (forward); 5'-TGAACATGTGCCACCAAAGT-3' (reverse)). The reagents used were from the ABsolute qPCR syber green mix (Abgene, Rochester, NY). The reaction conditions employed were: 95°C for 10 min followed by 40 periods of 96°C for 10 s, 55°C for 15 s, 72°C for 20 s and an 83°C/83°C/85°C/83.5°C/83°C cycle for 10 s. The reactions were analyzed in a Rotor Gene RG 3000 apparatus (Corbett LifeScience, Sydney, Australia) and estimates of up- and down-regulation of gene expression were obtained using the Relative Expression Software Tool (Corbett LifeScience).

Protein separation by two-dimensional electrophoresis (2-DE)

Protein extractions (70 μg) were desalted by passage over DG10 columns (Bio-Rad, Hercules, CA), dissolved in 2D buffer (6 M Urea, 2 M thiourea, 2% Chaps, 50 mM DTT, 0.2% Bio-Lyte), and cap-loaded onto rehydrated IPG strips (7 cm, pH 5–8, Bio-Rad) using a constant voltage of 50 mV for 2 h at room temperature. Proteins were separated according to p*I* values by applying a linear, sloping voltage enhancement first to 250 V over 30 min and then to 4,000 V over 2 h. This was followed by a rapid increment in voltage rate to a total of 10,000 V/h. The maximal current was limited to 50 μA/IPG strip. Strips were then frozen at −70° C for 30 min to break the gel and thawed for 15 min at 25° C. Subsequently, the strips were agitated for 10 min in DTT solution (100 mM) and in iodoacetamide solution (20 mM) for an additional 10 min at room temperature. Next, the treated strips were placed on top of a 4% SDS-PAGE stacking gel and allowed to enter a 12% of SDS-PAGE separating gel at 200 V for 2 h. Molecular weight markers in the range of 10–250 kDa were loaded next to the strip. Finally, the gels were stained by Sypro-Ruby (Invitrogen, Carlsbad, CA).

In-gel enzymatic digestion and mass spectrometry

The proteins of interest were excised from the 2-D gels, washed three times in double distilled water and the gel pieces were dehydrated in 100% acetonitrile (ACN) for 5 min and dried for 30 min in a vacuum centrifuge. Digestion was performed by adding 100 ng of modified trypsin (Promega, Madison, WI) in 200 mM ammonium bicarbonate. Following enzymatic digestion overnight at 37°C, the peptides were extracted with 50 μl of 60% ACN in 1% trifluoroacetic acid (TFA). The samples were dried and the peptides were purified using C_{18} zip-tips (Millipore, Bedford, MA).

The peptide mixtures (0.5 μl) were combined with a saturation solution of α-cyano-4-hydroxycinnamic acid

(0.5 μl, Bruker Daltonics, Bremen, Gemany) in ACN containing 1% TFA. The mixtures were analyzed by matrix-assisted laser desorption ionization time-of-flight mass spectrometry (MALDI-TOF MS, Bruker Daltonics) with peptide standards (Bruker Daltonics) used to calibrate the spectra. The mass results obtained by X-Mass software (Bruker Daltonics) were compared with the tryptic digestion protein sequence database (NCBI) using the MASCOT search engine (www.matrixscience.com, Matrix Science, London, UK), where a mass tolerance of 0.2 Da was chosen. For MS/MS identification, selected peptides identified in each spot were cleaved by GPMAW software and fragments were matched by MS-Tag search using the ProteinProspector search engine (prospector.ucsf.edu, UCSF, San Francisco, CA).

Immunoblotting of HSPs

Protein mixtures extracted from the membrane (fibrosarcoma cells) or the cytosol (fibroblast cells) were run on 10% SDS-PAGE at 180 V for 45 min, then trans-blotted onto nitrocellulose membranes for 1 h at 100 V (transfer buffer: 25 mM Tris, pH 7.4, 190 mM glycine, 20% methanol). Subsequent to 1 h blocking in 3% bovine albumin dissolved in blotting buffer (10 mM Tris-HCl, pH 7.4, 100 mM NaCl and 0.05% Tween) at room temperature, the blots were incubated for 1 h with anti-mouse HSP65, anti-rabbit grp78 and grp75, and anti-rat grp94 antibodies (Calbiochem, San Diego, CA, with the anti-grp antibodies being cross-reactive with mouse grps) at a concentration of 1 μg/ml in blotting buffer. The blots were washed three times for 20 min each and incubated in goat anti-mouse IgG-conjugated alkaline phosphatase (1:10,000, Calbiochem) for an additional 1 h at room temperature. Antibody binding was detected using the NBT reagent (Pierce, Rockford, IL).

Immunocytometry of HSPs and fluorescent staining of nuclei and actin

Cells (1×10^4) were cultured on sterile glass coverslips for 48 h, then washed and fixed in 4% formaldehyde in PBS for 15 min at room temperature, washed three times in PBS, and blocked in 1% fish gelatin (FSG) in PBS-Tween solution for an additional 30 min. Next, a series of cultured coverslips were incubated with anti-grp94, -grp78, -HSP70 and -HSP60 antibodies (5 μg/ml, Calbiochem) in PBS containing 0.2% FSG for 1 h at room temperature with gentle agitation, followed by incubation with (1:500) anti-rat IgG-conjugated Cy5 (for grp 78, anti-rabbit IgG Cy5 were used; Jackson ImmunoResearch, West Grove, PA) in PBS containing 0.2% FSG for 1 h at room temperature. Incubation with the secondary antibodies alone served as a negative control. Fluorescent staining of actin filaments and nuclei was carried out on the same coverslips to acquire a clear picture of HSP distribution within the cell. For actin staining, the cultured coverslips were incubated in (1:500) Oregon Green 488 phalloidin (Invitrogen) in PBS containing 0.2% FSG for 1 h at room temperature, then washed three times. For nuclear staining, the cultured coverslips were incubated in (1:1000) Hoechst dye (Invitrogen) in PBS containing 0.2% FSG for 1 h at room temperature and then washed three times. Finally, all coverslips were placed on slides containing 50% glycerol and inspected with an inverted microscope equipped with an Olympus IX81 camera, using appropriate fluorescent filters (Olympus, Center Valley, PA).

Tagging surface proteins by biotinylation

Cell cultures at 80% confluence were washed twice with 10 mL ice-cold PBS and incubated for 2 h at 4°C with Sulfo-NHS-Biotin Reagent (2 mM in PBS, pH 7.5, Pierce), as previously described [13]. Briefly, the reaction was terminated by the addition of 50 mM Tris-HCl, pH 7.5. The cells were then washed three times in 100 mM glycine to remove excess biotin reagent, after which cytosolic and membrane proteins were extracted as described above. The solubilized proteins were purified on ImmunoPure-immobilized streptavidin columns (Pierce) using the protocol supplied by the manufacturer.

Separation of charged glycans and their analysis in normal phase HPLC

According to the procedure of Küster *et al*. [14], PNGase-F-released glycans from the 2-D gels were fluorescently labeled with 2-AB by reductive amination. Subsequent to their labeling, the charged glycans were separated by anionic exchange on a 4.6×250 mm Vydac VHP301 column (Chromatech, Canton, MI) using two Waters 510 pumps, a Waters 717 autoinjector, and a FP-920 fluorescent detector (Jasco, Easton, MD). The solvents used were buffer A (50 mM ammonium formate, pH 9) and DDW, and elution was done by linear gradient over the course of 60 min. Initial conditions were 0% buffer A and 100% DDW at a flow rate of 1 ml/min and ending conditions were 80% buffer A and 20% DDW at the same flow rate. The column was washed with 100% A for 5 min at a flow rate of 1 ml/min before re-equilibration in the initial solvent system. Labeled fetuin glycans were used to determine the net charge of the samples. The eluted charged and uncharged glycans in volumes of 0.25 ml were collected manually into vials and then concentrated using a vacuum centrifuge. The Neu5Ac residues were digested from the charged glycans by overnight incubation with 1 μl of ABS (α 2- 3, 6, 8, 9- Neuraminidase, 1 U/ml, Prozyme, San Leandro, CA) in 50 mM of Tris-HCl, pH 5.5, and then

purified. The digested and uncharged glycans were separated in normal phase on a 4.6×250 mm Glyco-Sep N column (Waters, Milford, MA). The solvents used were buffer B (50 mM ammonium formate, pH 4.4) and buffer C (acetonitrile). The glycans were eluted by linear gradient with buffer B, such that initial conditions were 20% buffer B at a flow rate of 0.4 ml/min. The concentration of buffer B was changed from 35 to 53% over 132 min, and then from 53 to 100% over the next 3 min, with a constant flow rate. The column was washed with 100% buffer B for 5 min at a flow rate of 1 ml/min before re-equilibration in the initial solvent system.

Results

Expression of glycan epitopes and ST6Gal I transcripts in 3-MCA-induced fibrosarcoma cells

We compared the patterns of surface glycan expression on progressively-growing and non-invasive 3-MCA-induced cell lines obtained from either control BALB/c or IL-1$\alpha^{-/-}$ mice, respectively. Two cell lines from each phenotype were compared. Initially, we examined the patterns of lectin binding to cells. Accordingly, cells were stained with FITC-labeled lectins, *i.e*., Con A, WGA, PNA, Jacalin, RCA-I, and SNA, and then evaluated by flow cytometry. Con A binds α-linked mannose residues, WGA is a GlcNAc- and sialic acid-specific lectin, PNA binds β-galactosyl residues with strong reactivity to T-antigen (Galβ1-3GalNAcα1-Ser/Thr), Jacalin binds β-galactosyl residues and is specific for sialylated/neutral T-antigen, RCA-I binds β-galactosyl groups, and SNA is specific to α2-6 Neu5Ac residues [15]. The left graphs of Fig. 1a show the lectin binding differences between cell lines derived from 3-MCA-treated control mice and those derived from similarly treated IL-1$\alpha^{-/-}$ mice. Significant differences in the binding of SNA and PNA were observed between both types of fibrosarcoma cells, whereas no differences were observed in the binding of Jacalin (Fig. 1a), Con A, WGA or RCA-I (results not shown for Con A, WGA, or RCA-I). Quantitatively, binding to the surface of progressively growing fibrosarcoma cells was observed to increase by 3-fold for SNA and to decrease by 3-fold for PNA relative to their binding to regressing fibrosarcoma cells. Although the increase in SNA binding is consistent with the decrease in PNA binding, the latter could be inhibited by Neu5Ac residues linked not only through α2-6, but also those linked through α2-3 and α2-8. In contrast, Jacalin, which binds similar epitopes to those bound by PNA, was also bound to the surfaces of both cell types, as the Neu5Ac residues do not interfere with the binding of β-galactosyl epitopes to Jacalin as they do in the case of PNA [15]. The binding of neuraminidase-treated cells to SNA was less than that observed before neuraminidase treatment and exhibited an insignificant shift between the two cell lines. Moreover, PNA binding after neuraminidase treatment increased by one order of magnitude more than that observed before treatment and in contrast to Jacalin, the binding to cells was the same before and after the treatment (Figure 1 in the supplementary data). PNA binding to cells is apparently inhibited by Neu5Ac residues in all the linkages.

To better understand the binding patterns of SNA, PNA, and Jacalin to fibrosarcoma cells, we compared their binding patterns in primary skin fibroblasts obtained from control and IL-1$\alpha^{-/-}$ mice. No significant differences in the binding patterns of the lectins to normal fibroblasts from either strain of mice were observed. This indicates that the observed alterations in lectin binding to fibrosarcoma cells are related to cell transformation (Fig. 1a, right graphs). It is notable that relative to primary fibroblasts from control and IL-1$\alpha^{-/-}$ mice, α2-6-linked Neu5Ac epitopes are increased by one order of magnitude in both types of fibrosarcoma cell lines.

Finally, we assessed the expression patterns of those glycosyltransferases that participate in protein glycosylation. Thus, ST3Gal VI, ST6GalNAc III, ST6Gal I (termed according to the nomenclature proposed by Tsuji *et al*. [16]) and α1, 3-GT mRNA levels were determined in two lines of progressively growing and two lines of regressing immunogenic fibrosarcoma cells by quantitative RT-PCR, using specifically designed primers. The transcription of ST6Gal I, the product of which attaches α2-6 Neu5Ac residues to the acceptor, Galβ1-4GlcNAc, in glycoprotein N-glycans, was significantly ($P<0.05$) up-regulated two-fold in progressively growing cells, relative to the level measured in regressing immunogenic fibrosarcoma cells (Fig. 1b). This result is consistent with the FACS analyses (Fig. 1a), pointing to enhanced expression and, possibly, activity of ST6Gal I.

Expression of mRNA encoding ST3Gal VI, which binds α2-3 Neu5Ac residues to the acceptor Galβ1-4GlcNAc on glycoproteins and glycolipids [17] was found to be similar in both lines, indicating the increased expression of very specific sialylated structures on progressively growing fibrosarcoma cells. In addition, in both cell lines, similar patterns of expression of mRNA for ST6GalNAc III, which links α2-6 Neu5Ac residues to Neu5Acα2-3Galβ1-3GalNAc acceptor molecules, and α1, 3-GT, which links galactosyl residues to Galβ1-4GlcNAc acceptor molecules, were observed.

HSP identification by MS and HSP immunoblotting

We adopted a membrane proteomics approach to identify surface HSPs that play roles in immunological events and

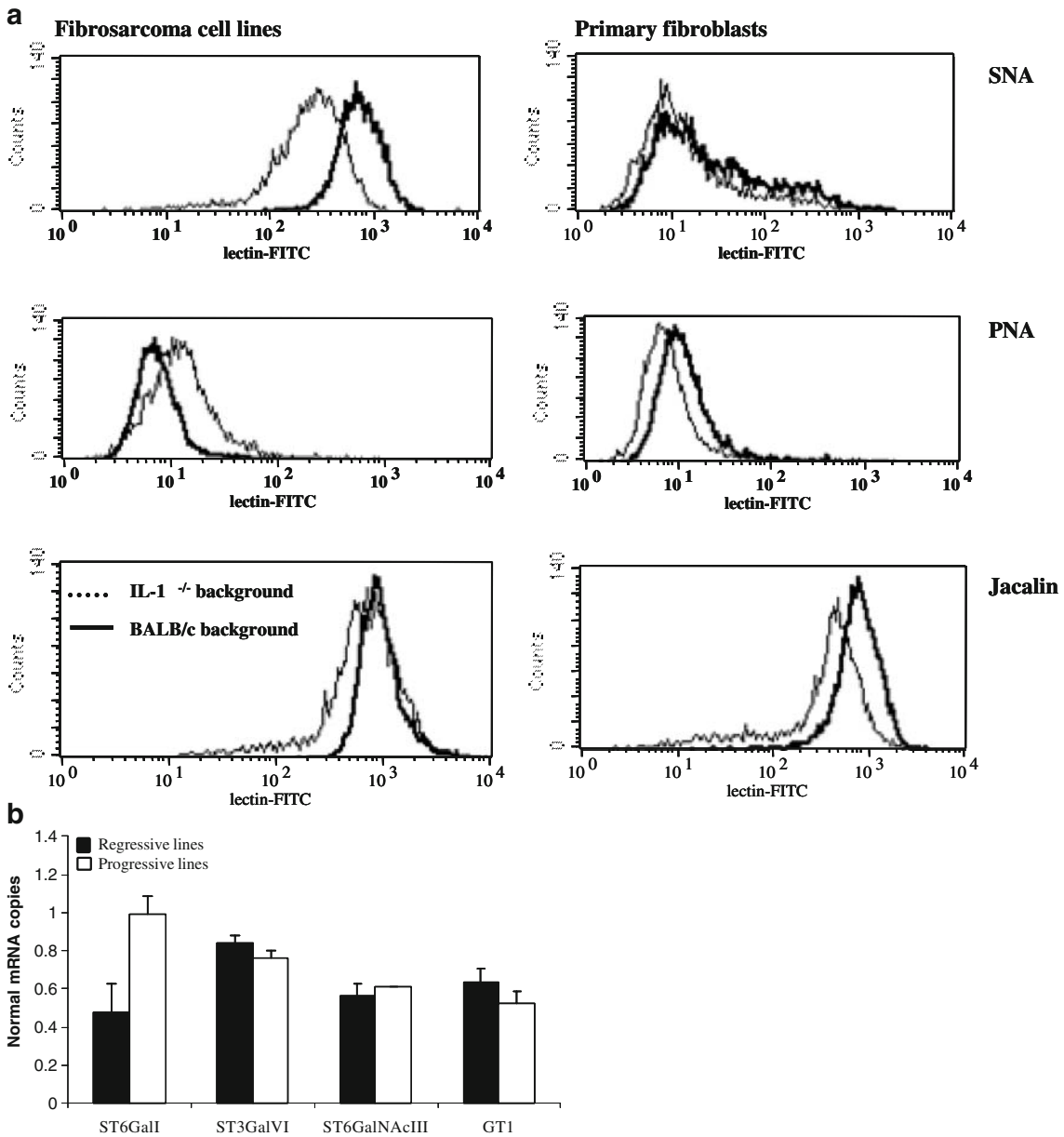

Fig. 1 Flow cytometry of regressive immunogenic and progressive fibrosarcoma cell lines derived from 3-MCA-injected IL-1$\alpha^{-/-}$ and BALB/c mice (left column) and flow cytometry of primary fibroblast cells derived from the skin of IL-1$\alpha^{-/-}$ and BALB/c mice (right column) stained by 30 μg/ml of fluorescent lectins, as described in Materials and Methods. SNA binds α2-6-linked Neu5Ac, PNA binds β-galactosyl residues that are strongly reactive to T-antigen, and Jacalin binds β-galactosyl residues and is highly specific for sialylated/neutral T-antigen (**a**). The mRNA levels of ST3Gal VI, ST6GalNAc III, ST6Gal I (nomenclature used is that proposed by Tsuji *et al*., ref 16) and a1, 3-GT were determined in two lines of regressive immunogenic and progressive fibrosarcoma cell lines by quantitative RT-PCR using specific primers. Statistical significance is considered $P<0.05$ versus the level of the housekeeping gene, β-actin (**b**)

that may contain different degrees of sialylation relative to fibrosarcoma cell line type. A typical membrane protein map of fibrosarcoma cells manifesting progressive growth patterns in mice, obtained by 2-DE and Sypro Ruby staining, exhibits proteins migrating between pI 5 to 8 and represents one of 5 membrane preparations of each cell line that was analyzed (Fig. 2a). Very similar protein maps were observed (results not shown) in the membrane preparation of regressing fibrosarcoma cell lines. We selected 29 protein spots, 80% of which were successfully identified by MALDI-TOF MS (Table 1) and confirmed by MS/MS sequencing using the MS-Tag software (Supplementary Data**,** Table 1). These spots represent a total of 6 different proteins, many of which were present as several isoforms,

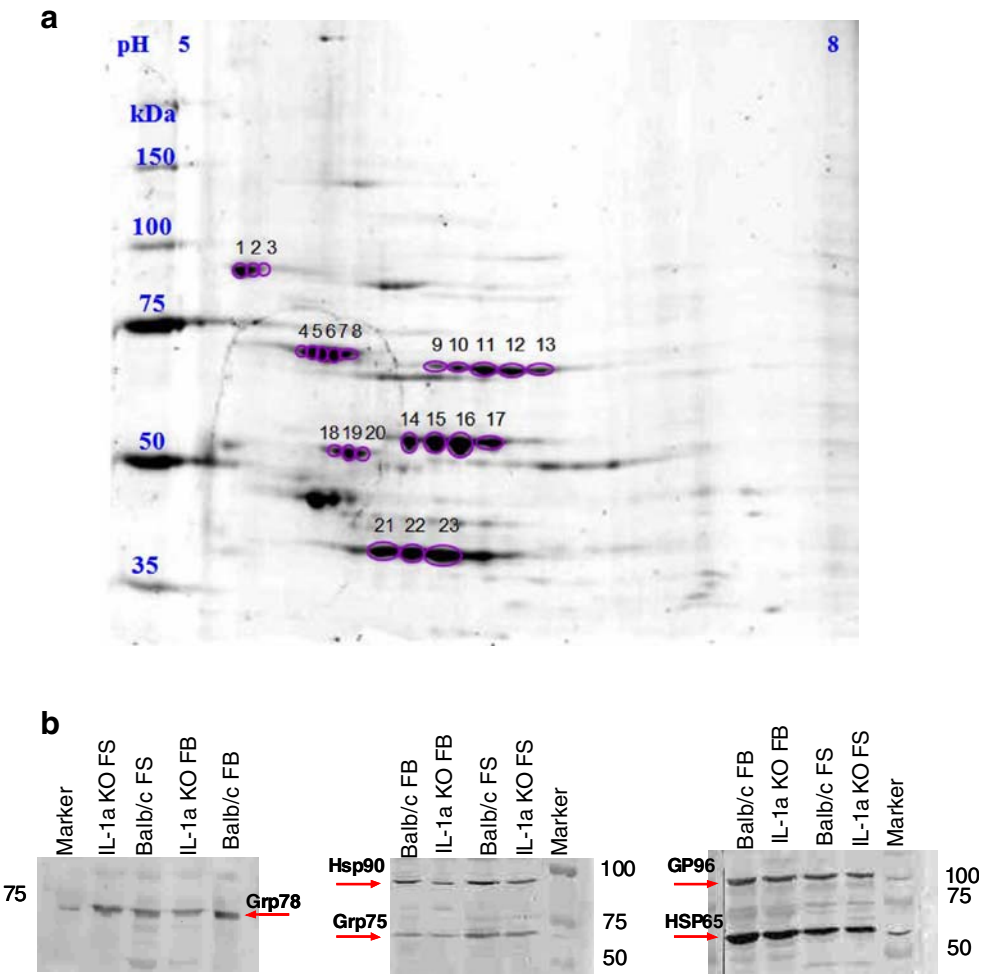

Fig. 2 2-DE image of membrane proteins extracted from progressive 3-MCA-induced fibrosarcoma cells using a ProteoExtract kit as described in Materials and Methods (**a**). Immunoblotting of HSP65, grp75, grp78, and gp96 using anti-mouse HSP65 and HSP90, anti-rabbit grp75 and grp78, and anti-rat grp94 antibodies, each at a concentration of 1 μg/ml per blot. HSPs were extracted from regressive immunogenic and progressive fibrosarcoma cells and from the cytosolic fraction of primary fibroblast cells derived from the skin of IL-1$\alpha^{-/-}$ and BALB/c mice (**b**). 1-DE of biotin-tagged HSPs extracted from the membranes of regressive immunogenic and progressive fibrosarcoma cell lines after tagging cell surface proteins by an impermeable biotin derivative (**c**). Immunocytometry of gp96 and fluorescent staining for nuclei and actin. Cells (1×10^4) were derived either from 3-MCA-induced fibrosarcoma cells injected into IL-1$\alpha^{-/-}$ and BALB/c mice or from primary fibroblast cells derived from the skin of IL-1$\alpha^{-/-}$ and BALB/c (**d**)

found at different pI values. Immunoblotting using anti-EGFR antibody confirmed that the protein preparation contained membrane proteins (Figure 2 in the supplementary data).

An analysis of the proteins from both types of fibrosarcoma cell lines showed a relative abundance of HSPs, which are increased in stressed cells, including malignant cells [18]. Three spots representing a molecular weight of 93 kDa and pI values of 5.22–5.26 matched grp94. Two series of five spots coinciding with a molecular weight of 72 kDa and pI values of 5.50–5.75 and a molecular weight of 69 kDa with pI values of 6.10–6.60 matched grp78 and grp75, respectively. Four spots corresponding to a molecular weight of 55 kDa and pI values of 6.05–6.40 matched HSP65. In addition, two cytoskeleton proteins were identified as β-tubulin and γ-actin. Tubulin was apparent in three spots of roughly 50 kDa and pI values of 5.05–5.15 and actin in three spots of roughly 40 kDa and pI values of 5.90–6.17.

The results of the MALDI-TOF MS analysis of HSP65, grp75, grp78, and gp96 were confirmed by immunoblotting using specific antibodies (Fig. 2b). In addition, these same reactions were performed on the total cytosolic protein pool extracted from primary skin fibroblasts obtained from control and IL-1$\alpha^{-/-}$ mice. As shown in Fig. 2b, the same HSPs that were apparent in the fibrosarcoma cells also appeared in the cytosolic protein pool. The intensities of the bands corresponding to fibroblast and fibrosarcoma HSPs were similar, due to the loading of equal protein concentrations.

HSPs presented a dot pattern, which was expected of glycoproteins; therefore, we chose to use HPLC for analyzing protein glycans. HPLC is not only a more sensitive method, but it also provides information on glycan composition and structure.

Localization and distribution of HSPs in 3-MCA-induced fibrosarcoma cells

Cell surface proteins were covalently modified by an impermeable biotin derivative that links to primary amino residues without inflicting cell damage [13]. Extracted biotinylated membrane proteins were isolated on a streptavidin affinity column and separated by SDS PAGE (Fig. 2c).

Fig. 2 (continued)

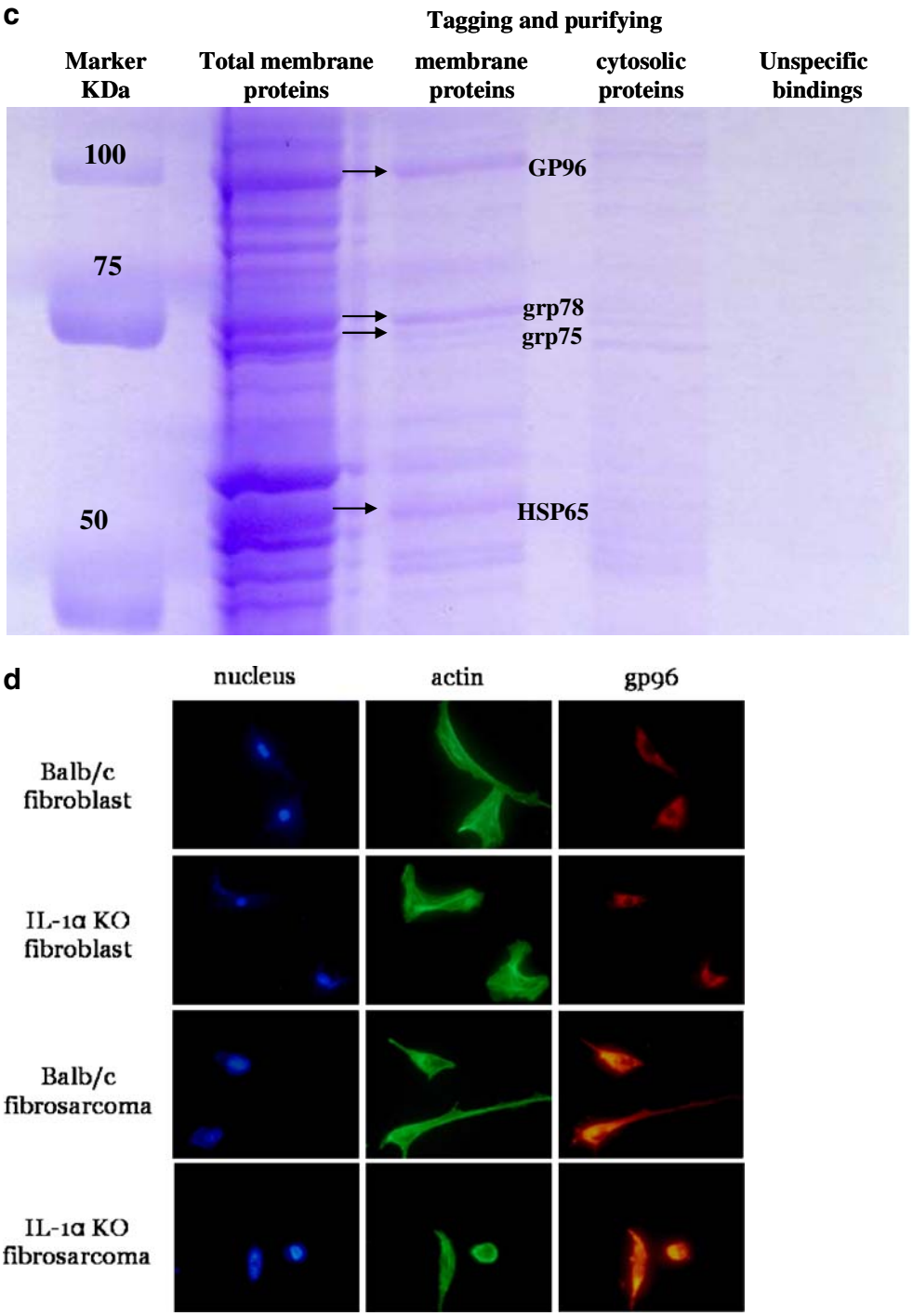

Membrane proteins HSP65, grp75, grp78, and gp96 from two lines of progressively growing and regressing fibrosarcoma were tagged and stained by Coomassie blue. The cytosolic proteins from both cultures were not tagged, and therefore, they were not stained. In addition, membrane HSPs were excised from the gels and their presence was confirmed by MALDI-TOF MS. Total untagged membrane proteins showed intense HSP bands, relative to the tagged bands. This was due to a loss of tagged proteins during purification and to sample contamination by traces of intracellular proteins during membrane protein recovery.

Non-permeabilized cells were immunofluorescence stained by anti-HSP antibodies, and nuclei and actin filaments of fibrosarcoma and primary fibroblast cells were also stained. Figure 2d shows that gp96 positively stained in all the cells examined, coinciding with the entire cell area of both types of fibrosarcoma. In primary fibroblasts from the skin of BALB/c and IL-1$\alpha^{-/-}$ mice, gp96 accumulated

Table 1 Proteins in dot patterns from membrane fractions of regressive and progressive fibrosarcoma cell lines developed in IL1$\alpha^{-/-}$ and WT mice identified by MALDI-TOF MS

Protein name	Accession no[a]	Spot no	Theoretical Mw/p*I*	Experimental Mw/p*I*	MASCOT score	Matched peptides	Sequence coverage (%)
Actin, gamma	gi|809561	21	41.3/5.56	40/5.90	112	10	29
Actin, gamma	gi|809561	22	42.1/5.31	40/6.05	106	16	46
Actin, gamma	gi|809561	23	41.3/5.56	40/6.17	130	11	37
Gp96	gi|6755863	1	92.7/4.74	93/5.22	130	17	22
Gp96	gi|6755863	2	92.7/4.74	93/5.24	82	9	15
Gp96	gi|6755863	3	92.7/4.74	93/5.26	36	7	10
Heat shock Protein 65	gi|51455	14	61.1/5.91	55/6.05	64	6	21
Heat shock Protein 65	gi|51455	15	61.1/5.91	55/6.15	100	11	25
Heat shock Protein 65	gi|51455	16	61.1/5.91	55/6.25	63	7	16
Heat shock Protein 65	gi|51455	17	61.1/5.30	55/6.40	91	10	23
Heat shock Protein 9	gi|162461907	9	73.7/5.81	69/6.10	60	7	11
Heat shock Protein 9	gi|162461907	10	73.7/5.81	69/6.25	82	7	14
Heat shock Protein 9	gi|162461907	11	73.7/5.81	69/6.35	37	5	10
Grp 75	gi|14917005	12	73.4/5.91	69/6.50	57	6	9
Grp 75	gi|162461907	13	73.4/5.91	69/6.60	66	7	11
Heat shock Protein 5	gi|31981722	4	72.5/5.01	72/5.50	178	22	39
Heat shock Protein 5	gi|31981722	5	72.5/5.01	72/5.55	242	23	48
Heat shock Protein 5	gi|31981722	6	72.5/5.01	72/5.60	194	17	35
BiP	gi|2598562	7	72.5/5.10	72/5.70	146	14	29
BiP	gi|2598562	8	72.5/5.10	72/5.75	127	13	27
Tubulin, beta	gi|21746161	18	50.4/4.78	50/5.05	28	6	11
Tubulin, beta	gi|21746161	19	50.4/4.78	50/5.10	53	9	20
Tubulin, beta	gi|21746161	20	50.4/4.78	50/5.15	66	11	25

[a] The number of the predicted protein in NCBInr

around the nuclei, as expected. Similar distribution patterns were observed for HSP65, grp75, and grp78 within the tumor lines, but with no accumulation in or around the nuclei (grp78) in primary fibroblasts (Supplementary Data, Figure 3a–c). Unlike the immunoblotting results, these results provide evidence of HSP over-expression in fibrosarcoma cells and suggest that the surfaces of fibrosarcoma cells were stained.

Different patterns of sialylated N-glycans on membrane HSPs

Our HSP analysis revealed that at least a fraction of this population may be glycosylated. The amino acid sequences of the different HSPs, as obtained from the SwissProt database, showed that HSP65, grp75, and gp96 can potentially be modified by N-glycans at 3 to 6 sites, as predicted by the presence of the consensus sequence, Asn-X-Ser/Thr (where X can be any amino acid except proline). No such motifs are present in grp78.

Chromatographic measurements and MALDI-TOF MS analysis of the N-glycans revealed oligomannose and complex type glycans in HSP65, grp75, and gp96. In particular, oligomannose sugars (Man_5-Man_9), both α1-6 fucosylated and a complex sialylated type, were identified on bi-, tri-, and tetra-antennary chains. In addition, some isomers of the tri- and tetra-antennary chains displayed// bisected GlcNAc residues (Avidan *et al.*, unpublished observations).

Next, the sialylated N-glycans of membrane HSPs were examined to distinguish the differences in these structures from progressively growing versus regressive tumor cell lines. Consequently, glycans were released, labeled, and separated by weak anion exchange (WAX) HPLC [14]. The eluted fractions of neutral, mono-, di-, and tri-sialylated glycans were collected at different time intervals and profiled by normal phase HPLC. Similar to a dextran ladder standard of different molecular weights, the times of glycan elution were expressed as glucose units (GU). A database of standard sugars assigned GU values established by Oxford Glycobiology Institute (http//glycobase.ucd.ie/cgi-bin/public/glycobase.cgi) was used in this study.

Table 2 summarizes the amount of charged glycans (in percentages), and Fig. 3 illustrates a comparative example

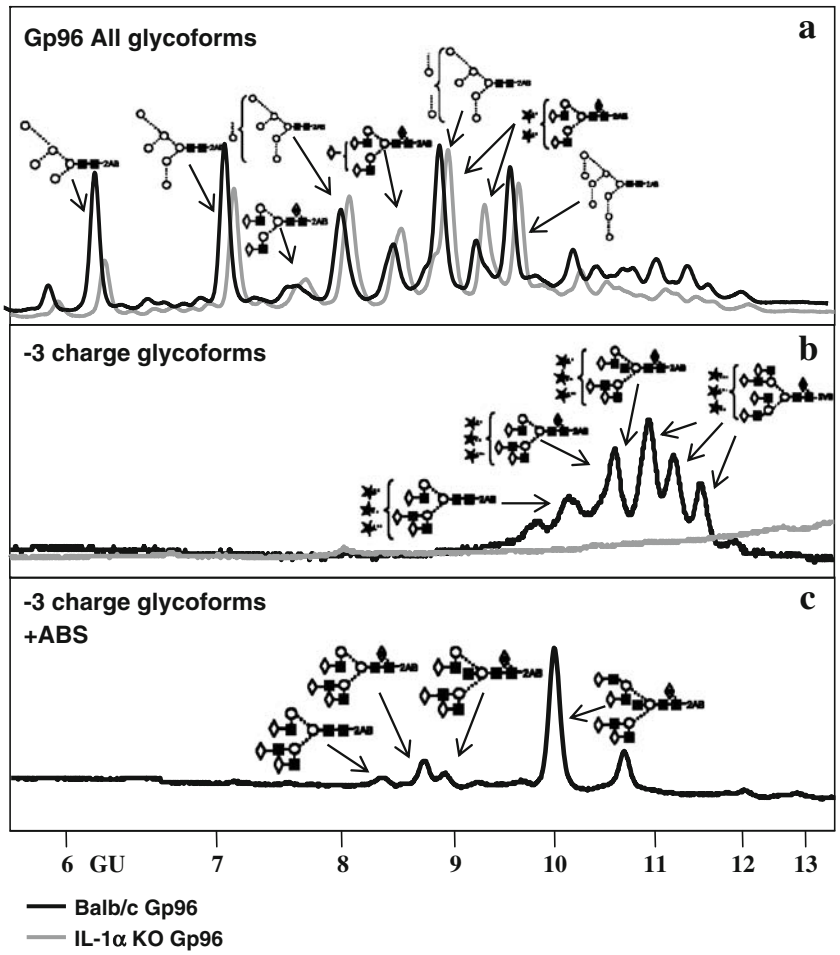

Fig. 3 NP-HPLC profiles of 2AB-labeled N-linked glycans from gp96 molecules from regressive immunogenic and progressive cells. Shown are intact glycans (**a**), trisialylated charged glycans (**b**), neuraminidase-(ABS) treated glycans from the trisialylated fraction (**c**), intact N-linked glycans from grp75 molecules from regressive immunogenic and progressive cells (**d**), trisialylated charged glycans (**e**) and neuraminidase-treated glycans from the trisialylated fraction (**f**) and N-linked glycans from HSP65 molecules from regressive immunogenic and progressive cells, the intact glycans (**g**), trisialylated charged glycans (**h**) and neuraminidase-treated glycans of the trisialylated fraction (**i**) ★ Sialic acid; ■ N-acetylglucosamine; ● Galactose; ◇ Fucose; ○ Mannose

of a trisialylated fraction (10–13 GU) attained upon profiling total intact glycans (Fig. 3a, d, g), intact charged glycans (Fig. 3b, e, h), and neuraminidase (ABS)-treated glycans of both fibrosarcoma lines (Fig. 3c, f, i). The trisialylated tetra-antennary glycans, bisected GlcNAc, and fucosylated and non-fucosylated triantennary glycans appeared in three different peaks. ABS-digestion shifted the peaks into the positions of neutral tetra-antennary and neutral tri-antennary glycans, respectively. Because ABS can concurrently cleave α 2-3, α 2-6, α 2-8, and α 2-9 Neu5Ac residues, use of this reagent confirmed the identities of the structures obtained. A comparison of average amounts of the charged structures (Table 2) indicated that trisialylated glycans were detected on gp96 of the progressive cells but not on the same protein in regressive cells. Similarly, two to four times more trisialylated glycans were present on HSP65 in the progressive cells than in the regressive cells. Additionally, the disialylated content of HSP65 in the progressive cells was eight times higher than in the regressive cells. By contrast, the grp75 sialylation profile of the progressive cells was two times lower than that of its counterpart in the regressive cells. Finally, monosialylated glycans on grp75 were detected at a level two to three times higher in the progressive cells than in the regressive cells.

Discussion

The integrated effects of innate and adaptive immunity were shown to affect the survival of malignant cells that develop in experimental tumorigenesis during the cancer immunoediting process. Previous studies revealed that in mice deficient in critical cells or cytokines—*i.e.*, lymphocytes, NKT cells, and IFNγ to name a few—the immunogenic variants of malignant cells are not eliminated during tumor progression, and as a result, the overt tumors consist of immunogenic cells that subsequently fail to develop into tumors when transplanted into secondary hosts [19–21]. Here, we employed 3-MCA-induced fibrosarcoma lines from IL-1$\alpha^{-/-}$ mice that had not been properly edited. As a result, they were immunogenic and induced regressing tumors [11]. Such cells, however, grow in immunocompromised hosts. In tumor cells developed in IL-1$\alpha^{-/-}$ mice, molecules that participate in antigen presentation and that favor interactions between immune cells—like MHC class

Fig. 3 (continued)

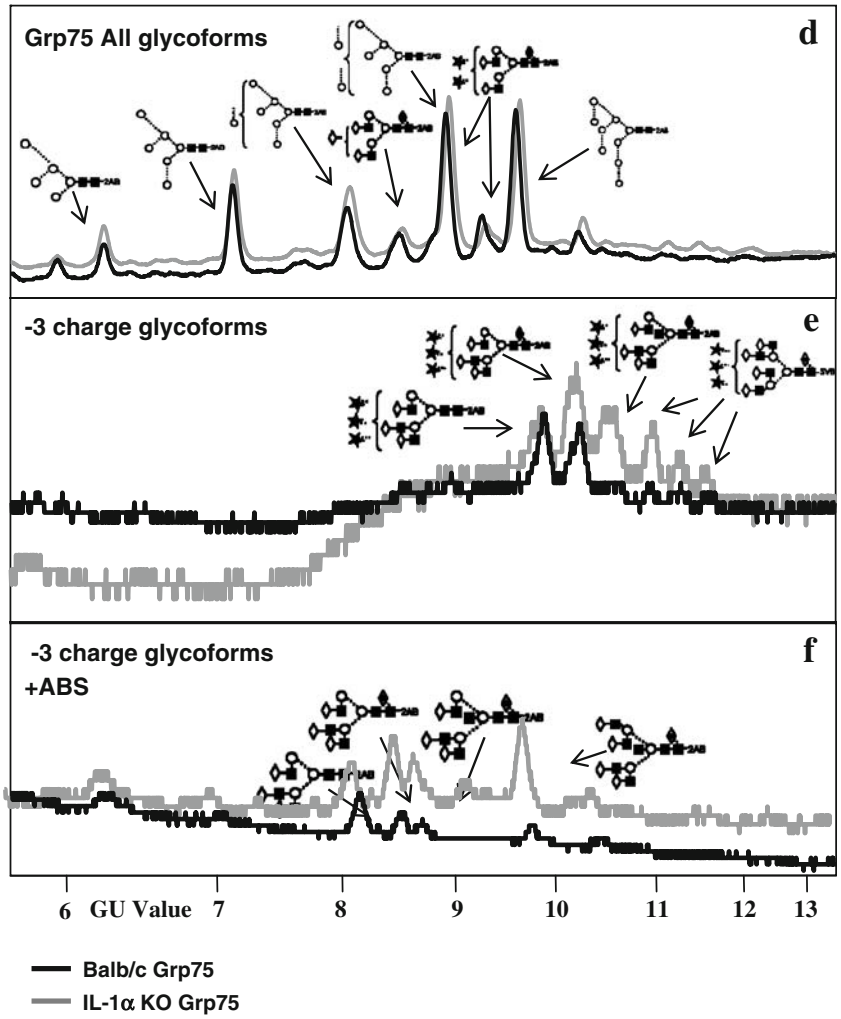

I, co-stimulatory, and adhesion molecules—are more abundantly expressed than on 3-MCA-induced cell lines derived from WT mice. In the present study, we associate molecules exhibiting aberrant glycans with the process of tumor immunoediting.

We have revealed that the expression of α2-6-linked Neu5Ac epitopes was abundant in progressively growing fibrosarcoma in comparison with regressing fibrosarcoma cell lines that are eradiated by immune mechanisms. Accordingly, up-regulation of ST6Gal-I expression was observed in progressively growing fibrosarcoma cells. In addition, the expression of α2-6-linked Neu5Ac epitopes in both types of fibrosarcoma cell lines was higher than in primary fibroblasts of the same lineage. Previous studies in several types of human carcinomas, and most recently in spontaneous cancer in ST6Gal-I$^{-/-}$ mice, have suggested that the upregulation of ST6Gal-I correlates with the effects of α2-6-linked Neu5Ac epitopes on metastatic spread, poor prognosis, and tumor progression via enhanced β-integrin function [4, 22, 23]. To the best of our knowledge, however, there have been no reports indicating that the enhancement of ST6Gal-I modulates the interactions of tumor cells with effector cells of the immune system. By contrast, over-sialylation of T- and Tn-antigens in MUC1 mucin—such as T47D, which is produced in metastatic breast carcinoma—was shown to contribute to tumor immunosuppression by increasing the amounts of secreted IL-10 and diminishing the production of IL-12 from dendritic cells [24].

Several possible explanations exist for the role of α2-6 Neu5Ac residues in determining tumor cell immunogenicity. On one hand, it is possible that ST6Gal-I modulates the interactions of tumor cells with the immune system. On the other hand, another enzyme or several enzymes acting simultaneously, from an assortment of sialyltransferases that exist in the cell, could also be altered to generate varied ligands, like GD3, the disialylganglioside that can modulate NK cell cytotoxicity via siglec-7 [25]. We found that removing surface Neu5Ac residues from progressively growing fibrosarcoma cells by neuraminidase did not affect the viability or in vitro proliferative capacity of the cells, but it did induce tumor regression upon injection into WT mice, a phenomenon related to eradication of the malignant cells by NK cells (unpublished observations).

Fig. 3 (continued)

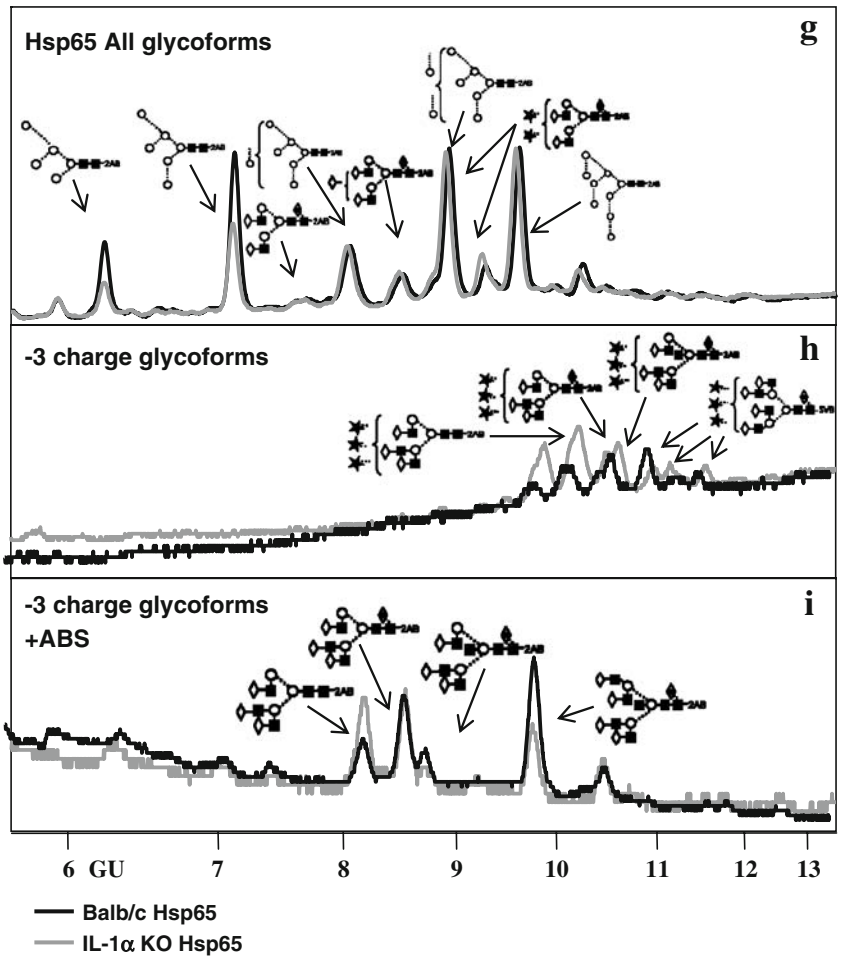

Impermeable tagging of the pool derived from the fractionated membrane proteins and MALDI analysis illustrated the distributions of HSP65, grp75, and gp96 on the cell surface, and immunofluorescent staining showed their distribution throughout the cell and their over-expression relative to their observed limited accumulation in primary fibroblast cells. However, we could not detect HSP expression on the cell membrane by FACS analysis, possibly due to the use of commercial anti-HSP antibodies, which may have limitations when used to identify intracellular HSPs. Traditionally, HSPs were thought to have been located in intracellular compartments, and accordingly with the exception of endoplasmic reticulum (ER) residents such as gp96 and grp78, which are able to transport to the Golgi as a consequence of their over-expression in the ER they do not contain a consensual secretory signal sequence [26]. Nonetheless, the appearance of HSPs on the surface membrane and within the ECM of viable malignant cells has been well documented [27–29]. The release of the cytosolic HSP70, for example, was shown via exosomes, via an endo-lysosomal-dependent pathway [28], and recently by Vega *et al*. through translocation into the plasma membrane before its release in a membrane-associated form to the extracellular environment [30]. Moreover, membrane-bound HSPs have been found to exhibit immunomodulatory potential [31–34]. A 14-mer peptide derived from tumor membrane-bound HSP70 was shown to stimulate NK cells [35], while surface gp96 enhanced the cross-presentation of antigens and the priming of tumor-specific T cells [36]. Similarly, Vega *et al*. conceived that HSP70 may exist in a multimeric form within the membrane, and as such, it could trigger an immune cell response. We assume that cytosolic HSPs in malignant cells can arise in an alternate form at the DNA sequence or transcription levels, directing the synthesis of HSPs through the ER-Golgi secretion pathway [37–39], where it would acquire glycans, thus affecting the immunological properties of the proteins. Accordingly, we detected sialylated glycans on the HSPs that were examined, attesting to their location on the membrane since Neu5Ac residues appear on surface and secreted glycoproteins [40].

A gross estimation based on a calculation of the amount of glycans produced from 1 mg of recovered protein indicated that less than 10% of the HSPs were glycosylated.

Table 2 Charged N-glycans of cell surface gp96, grp75, and HSP65 extracted from regressive and progressive fibrosarcoma cell lines

Name	Structure	GU	Gp96		Hsp65		Grp75	
			BALB/c	IL-1α KO	BALB/c	IL-1α KO	BALB/c	IL-1α KO
FcA4G4S3	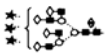	11.541, 11.244, 10.925	1.17%	ND	1.51%	0.88%	0.86%	0.58%
FcA3G3S3	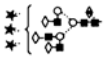	10.049	0.68%	ND	1.06%	0.26%	0.35%	0.81%
FcA3BG3S3	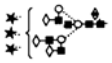	10.492	0.85%	ND	1.25%	0.35%	0.57%	ND
A3G3S3		9.634	0.28%	ND	0.35%	0.11%	ND	0.92%
FcA2G2S2		9.517, 9.130, 8.722	7.00%	3.28%	4.79%	0.63%	2.27%	4.20%
A2G2S2	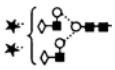	8.337, 7.970	2.56%	4.06%	1.61%	0.21%	1.40%	2.20%
FcA4G4S2	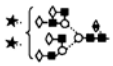	10.746	0.84%	ND	0.28%	0.03%	ND	ND
FcA3G3S2	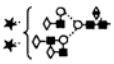	9.685	1.63%	1.23%	0.57%	0.08%	0.28%	0.55%
FcA3BG3S2	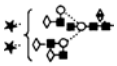	10.08	1.09%	1.65%	ND	ND	ND	0.18%
A3G3S2	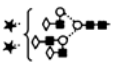	9.261	1.33%	2.31%	ND	ND	0.66%	0.93%
A3G2S2		8.361	0.46%	ND	ND	ND	ND	ND
FcA2G2S1	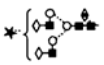	8.359, 7.941	13.51%	12.03%	5.46%	2.05%	7.02%	3.23%
A2G2S1	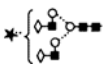	7.562	2.46%	2.53%	0.50%	1.24%	1.78%	0.72%

Sequencing the N-glycans found on HSP65, grp75, and gp96 revealed high mannose and complex glycan contents. The sialylated glycans were shown to carry terminating mono-, di-, and tri- Neu5Ac residues on 2–4 antennas assembled on complex type N-glycans. Thus far, the few studies on HSP glycosylation that have been conducted mainly addressed intracellular HSPs, especially gp96, which bears high numbers of mannose glycans, or the dynamic β-O-GlcNAc glycosylation of HSP70 [41, 42]. An interaction between hyperglycosylated gp96 in the ER and either of the Toll-like receptors (TLRs), 4 or 9, was shown to induce rapid folding of TLR molecules in macrophages. Gp96-deficient mice were shown to be resistant to endotoxin-shock due to a lack of functional TLR 4, indicating that gp96 is a master chaperone for this TLR molecule [43].

We expected to observe differences in the expressions of sialylated HSPs between malignant cells derived from WT mice and those from IL-1$\alpha^{-/-}$ mice, assuming that HSPs bearing low levels of sialylated glycans can trigger an immune response. The low expressions of gp96 and HSP65 trisialylated N-glycans in regressive fibrosarcoma cells and of disialylated HSP65 glycans and monosialylated grp75 glycans in regressive cells indicated that specific glycoforms bear low levels of sialylated glycans. Indeed, substantial amounts of one type of glycoform could influence glycoprotein function [44], such that a low amount of sialylated N-glycans may induce an immune response. Suriano *et al.* were the first to suggest a relationship between gp96 glycan epitopes and cell phenotype, specifically gp96 function [41]. We supported their hypothesis by characterizing the differences between the arrays of sialylated HSP glycans expressed on a series of regressive, immunogenic cell lines and the progressive, non-immunogenic cell lines that were concomitantly induced by a chemical carcinogen in strains of mice differing in their immunosurveillance potential to detect emerging malignant cells during tumor progression (cancer immunoediting). It is noteworthy that no HSPs were detected on the surface of primary dermal fibroblasts, which were the target cells of transformation in our experimental system of

chemical carcinogenesis. This hints that, indeed, the expression of surface HSPs and their glycosylation are a result of immunosurveillance that occur during tumor progression. However, we do not yet understand the exact physiological contribution of different sialylated HSP glycans in determining their immunogenicity or invasiveness.

In conclusion, the 3-MCA-induced fibrosarcoma cell lines that arise in IL-1α-deficient mice provide evidence for restricted levels of α2-6 Neu5Ac residues in tumors eradicated by the immune system by selecting for immunogenic variant tumor cells. The degree of sialylation of N-glycans on membrane HSPs is a function of the glycoform amounts which, therefore, determine the immunogenic properties of the HSPs. Thus, sialylation of 3-MCA-induced fibrosarcoma cells is a complex, controlled process that may affect the immunogenicity of malignant cells. Further studies are needed to characterize the pattern and physiological relevance of glycosylated and sialylated HSPs on tumor cells.

Acknowledgements The authors thank Dr. Uri Abdu for his help in carrying out fluorescent staining and microscopic imaging and Dr. Yoram Tekoah for helpful advice on glycan analysis by HPLC. This work was supported in part by the Israel Cancer Association and by the Israeli Glycobiology Center of Ben-Gurion University of the Negev, Israel.

References

1. Dube, D.H., Bertozzi, C.R.: Glycans in cancer and inflammation-potential for therapeutics and diagnostics. Nat. Rev. Drug Discov. **4**, 477 (2005). doi:10.1038/nrd1751
2. Fuster, M.M., Esko, J.D.: The sweet and sour of cancer: glycans as novel therapeutic targets. Nat. Rev. Cancer. **5**, 526 (2005). doi:10.1038/nrc1649
3. Dall'olio, F., Chiricolo, M., Altimari, A., Fiorentino, M., Grigioni, W.F.: Expression of β-galactoside sialyltransferase and of α2, 6-sialyltransferase glycoconjugates in normal human liver, hepatocarcinoma and cirrhosis. Glycobiol. **14**, 39–49 (2004). doi:10.1093/glycob/cwh002
4. Dall'olio, F., Chiricolo, M.: Sialyltransferases in cancer. Glycoconj. **18**, 841 (2001). doi:10.1023/A:1022288022969
5. Wang, P.H.: Altered glycosylation in cancer: sialic acids and sialyltransferases. J. Cancer Mol. **1**, 73 (2005)
6. Seidenfaden, R., Krauter, A., Schretzinger, F., Gerardy-Schahn, R., Hildebrandt, H.: Polysialic acid directs tumor cell growth by controlling heterophilic neural cell adhesion molecule interactions. Mol. Cell. Biol. **23**, 5908 (2003). doi:10.1128/MCB.23.16.5908-5918.2003
7. Swann, J.B., Smyth, M.J.: Immune surveillance of tumors. J. Clin. Invest. **117**, 137 (2007). doi:10.1172/JCI31405
8. Dunn, G.P., Koabel, C.M., Schreiber, R.D.: Interferons, immunity and cancer immunoediting. Nat. Immunol. **6**, 836 (2006). doi:10.1038/nri1961
9. Apte, R.N., Dotan, S., Elkabets, M., White, R.M., Reich, E., Carmi, Y., Son, X., Dvozkin, T., Kerlin, Y., Voronov, E.: The involvement of IL-1 in tumorigenesis, tumor invasiveness, metastasis and host-interaction. Cancer Metastasis. Rev. **25**, 387 (2006). doi:10.1007/s10555-006-9004-4
10. Krelin, Y., Voronov, E., Dotan, S., Elkabets, M., Reich, E., Fogel, M., Huszar, M., Iwakura, Y., Segal, S., Dinarello, C.A., Apte, R. N.: IL-1 beta-driven inflammation promotes the development and invasiveness of chemical carcinogen-induced tumors. Cancer Res. **67**, 1062 (2007). doi:10.1158/0008-5472.CAN-06-2956
11. Elkabets, M., Krelin, Y., Dotan, S., Cerwenka, A., Porgador, A., Lichtenstein, R.G., Dinarello, C.A., White, M.R., Zoller, M., Voronov, E., Apte, R.N.: Host-derived Interleukin-1α is important in determining the immunogenicity of 3-Methylcholantrene-tumor cells. J. Immunol. **182**, 4874 (2009)
12. Gorelik, E., Xu, F., Henion, T., Anaraki, F., Galili, U.: Reduction of metastatic properties of BL6 melanoma cells expressing terminal fucose(alpha) 1–2-galactose after alpha1, 2-fucosyltransferase cDNA transfection. Cancer Res. **57**, 332 (1997)
13. Shin, B.K., Wang, H., Yim, A.M., Le Naour, F., Brichory, F., Jang, J.H., Zhao, R., Puravs, E., Tra, J., Michael, C.W., Misek, D. E., Hanash, S.M.: Global profiling of the cell surface proteome of cancer cells uncovers an abundance of proteins with chaperone function. J. Biol. Chem. **278**, 7607 (2003). doi:10.1074/jbc.M210455200
14. Küster, B., Wheeler, S.F., Hunter, P.A., Dwek, R.A., Harvey, D.J.: Sequencing of N-glycan oligosaccharides directly from protein gels: In gel deglycosylation and analyzing in HPLC and MALDI-TOF MS. Anal. Biochem. **250**, 82 (1997). doi:10.1006/abio.1997.2199
15. Van Damme, E.J.M., Peumans, W.J., Pusztai, A., Bardocz, S.: Handbook of plant lectins: properties and biomedical applications, 1st edn. Willey, England (1998)
16. Tsuji, S., Datta, A.K., Paulson, J.C.: Systematic nomenclature for sialyltransferases. Glycobiol. **6**, V (1996). doi:10.1093/glycob/6.7.647
17. Okajima, T., Fukumoto, S., Miyazaki, H., Ishida, H., Kiso, M., Furukawa, K., Urano, T., Furukawa, K.: Molecular cloning of a novel alpha2,3-sialyltransferase (ST3Gal VI) that sialylates type II lactosamine structures on glycoproteins and glycolipids. J. Biol. Chem. **274**, 11479 (1999). doi:10.1074/jbc.274.17.11479
18. Sherman, M., Multhoff, G.: Heat shock proteins in cancer. Ann. N. Y. Acad. Sci. **1113**, 192 (2007). doi:10.1196/annals.1391.030
19. Dunn, G.P., Bruce, A.T., Sheehan, K.C., Shankaran, V., Uppaluri, R., Bui, J.D., Diamond, M.S., Koebel, C.M., Arthur, C., White, J. M., Schreiber, R.D.: A critical function for type I interferons in cancer immunoediting. Nat. Immunol. **6**, 722 (2005). doi:10.1038/ni1213
20. Dunn, G.P., Bruce, A.T., Ikeda, H., Old, L.J., Schreiber, R.D.: Cancer immunoediting: from immunosurveillance to tumor escape. Nat. Immunol. Rev. **2**, 991 (2002)
21. Zitvogel, L., Tesniere, A., Kroemer, G.: Cancer despite immunosurveillance: immunoselection and immunosubversion. Nat. Immunol. Rev. **6**, 715 (2006). doi:10.1038/nri1936
22. Hedlund, M., Ng, E., Varki, A., Varki, N.M.: Alpha 2-6-Linked sialic acids on N-glycans modulate carcinoma differentiation in vivo. Cancer Res. **68**, 388 (2008). doi:10.1158/0008-5472.CAN-07-1340
23. Varki, N.M., Varki, A.: Diversity in cell surface sialic acid presentations: implications for biology and disease. Lab. Invest. **87**, 851 (2007). doi:10.1038/labinvest.3700656
24. Rughetti, A., Pellicciotta, I., Biffoni, M., Bäckström, M., Link, T., Bennet, E.P., Clausen, H., Noll, T., Hansson, G.C., Burchell, J.M., Frati, L., Taylor-Papadimitriou, J., Nuti, M.: Recombinant tumor-associated MUC1 glycoprotein impairs the differentiation and function of dendritic cells. J. Immunol. **174**, 7764 (2005)
25. Nicoll, G., Avril, T., Lock, K., Furukawa, K., Bovin, N., Crocker, P.R.: Ganglioside GD3 expression on target cells can modulate NK cell cytotoxicity via siglec-7-dependent and -independent mechanisms. Eur. J. Immunol. **33**, 1642 (2003). doi:10.1002/eji.200323693

26. Lewis, M.J., Pelham, H.R.: Ligand-induced redistribution of a human KDEL receptor from the Golgi complex to endoplasmic reticulum. Cell. **68**, 353 (1992). doi:10.1016/0092-8674(92)90476-S
27. Altmeyer, A., Maki, G.R., Feldweg, A.M., Heike, M., Protoprov, V.P., Masur, S.K., Srivastava, P.K.: Tumor-specific cell surface expression of the –KDEL containing, endoplasmatic reticular heat shock protein gp96. Int. J. Cancer. **69**, 340 (1996). doi:10.1002/(SICI)1097-0215(19960822)69:4<340::AID-IJC18>3.0.CO;2-9
28. Multhoff, G.: Heat shock protein 70 (HSP70): membrane location, export and immunological relevance. Methods. **43**, 229 (2007). doi:10.1016/j.ymeth.2007.06.006
29. Robert, J., Menoret, M., Cohen, N.: Cell surface expression of the endoplasmatic reticular heat shock protein gp96 is phylogenetically conserved. J. Immunol. **163**, 4133 (1999)
30. Vega, V.L., Rodríguez-Silva, M., Frey, T., Gehrmann, M., Diaz, J. C., Steinem, C., Multhoff, G., Arispe, N., De Maio, A.: Hsp70 translocates into the plasma membrane after stress and is released into the extracellular environment in a membrane-associated form that activates macrophages. J. Immunol. **180**, 4299 (2008)
31. Lee, A.S.: GRP78 induction in cancer: therapeutic and prognostic implications. Cancer Res. **67**, 3496 (2007). doi:10.1158/0008-5472.CAN-07-0325
32. Srivastava, P.K.: Interaction of heat shock proteins with peptides and antigen presenting cells: chaperoning of the innate and adaptive immunity. Annu. Rev. Immunol. **20**, 395 (2002). doi:10.1146/annurev.immunol.20.100301.064801
33. Broere, F.H., Weiten, L., Zee, R.V.D., Berlo, S.: Heat shock proteins induce T cell regulation of chronic inflammation. Ann. Rheum. Dis. **65**, 65 (2007)
34. Doody, A.D.H., Kovalchin, T.J., Mihalyo, M.A., Hagymasi, A.T., Drake, C.G., Adler, A.J.: Glycoprotein 96 can chaperone both MHC class I- and class II-restricted epitopes for in vivo presentation, but selectively primes CD8 + T cell effector function. J. Immunol. **172**, 6087 (2004)
35. Multhoff, G., Pfister, K., Gehrmann, M., Hantschel, M., Gross, C., Hafner, M., Hiddemann, W.: A 14-mer Hsp70 peptide stimulates natural killer (NK) cell activity. Cell Stress Chaperones. **6**, 337 (2001). doi:10.1379/1466-1268(2001)006<0337:AMHPSN>2.0.CO;2
36. Dai, J., Liu, B., Caudill, M.M., Zheng, H., Qiao, Y., Podack, E.R., Li, Z.: Cell surface expression of heat shock protein gp96 enhances cross-presentation of cellular antigens and the generation of tumor-specific T cell memory. Cancer Immun. **3**, 1 (2003)
37. Hwang, E.M., Kim, D.G., Lee, B.J., Choi, J., Kim, E., Park, N., Kang, D., Han, J., Choi, W.S., Hong, S.G., Park, J.Y.: Alternative splicing generates a novel non-secretable cytosolic isoform of NELL2. Biochem. Biophys. Res. Commun. **353**, 805 (2006). doi:10.1016/j.bbrc.2006.12.115
38. Unoki, M., Shen, J.C., Zheng, Z.M., Harris, C.C.: Novel splice variants of ING4 and their possible roles in the regulation of cell growth and motility. J. Biol. Chem. **281**, 34677 (2006). doi:10.1074/jbc.M606296200
39. Pyhtila, B., Zheng, T., Lager, P.J., Keene, J.D., Reedy, M.C., Nicchitta, C.V.: Signal sequence- and translation-independent mRNA localization to the endoplasmic reticulum. RNA. **14**, 445 (2008). doi:10.1261/rna.721108
40. Varki, A.: Glycan-based interactions involving vertebrate sialic-acid-recognizing proteins. Nature. **443**, 1023 (2007). doi:10.1038/nature05816
41. Suriano, R., Ghosh, S.K., Ashok, B.T., Mittelman, A., Chen, Y., Banerjee, A., Tiwari, R.K.: Differences in glycosylation patterns of heat shock protein, gp96: implications for prostate cancer prevention. Cancer Res. **65**, 6466 (2005). doi:10.1158/0008-5472.CAN-04-4639
42. Guinez, C., Lemoine, J., Michalski, J.C., Lefebvre, T.: 70-Kda-heat shock protein presents an adjustable lectinic activity towards O-linked N-acethylglucosamine. Biochem. Biophys. Res. Commun. **319**, 21 (2004). doi:10.1016/j.bbrc.2004.04.144
43. Yang, Y., Liu, B., Dai, J., Srivastava, P.K., Zammit, D.J., Lefrancois, L., Li, Z.: Heat shock protein gp96 is a master chaperone for toll-like receptors and is important in the innate function of macrophages. Immunity. **26**, 1 (2007). doi:10.1016/j.immuni.2006.12.005
44. Dwek, R.A.: Glycobiology: toward understanding the function of sugars. Chem. Rev. **96**, 683 (1996). doi:10.1021/cr940283b